PHYSICAL REVIEW B VOLUME 23, NUMBER 8 15 APRIL 1981

Retarded coupling constants of fast electrons to surface polaritons of thin films

W. Ekardt
Fritz-Haber-Institut der Max-Planck-Gesellschaft, Faradayweg 4-6, D-1000 Berlin 33, Germany
(Received 8 September 1980)

The coupling of electrons to surface modes of a metallic or dielectric slab has been derived with full inclusion of retardation. A detailed comparison of the retarded scattering efficiency to the nonretarded one shows clearly that small-angle scattering is governed by retardation effects. At high electron energies and small angles of incidence the retarded cross section differs from the nonretarded one by some orders of magnitude in the whole region $0 \leq q \leq \omega_p/c$, where q is the wave vector of the surface polariton, and ω_p is the plasma frequency. The coupling constants are then applied to retarded *multiple scattering* of fast electrons by surface polaritons and compared with the nonretarded results. We show that multiple scattering by the dispersive part of surface polaritons or plasmons, respectively, plays an important role in case of thin metallic slabs.

I. INTRODUCTION

Ten years ago the coupling of electrons to surface modes was worked out systematically by a number of authors.[1-6] Common to all this work is the neglect of retardation, mainly because the theory then is simplified to a great extent. Only qualitative arguments are given for the justification of this neglect, mainly based on phase space arguments.[5,7] The theory in its simplified form has been applied to a number of related problems: the image potential problem,[8] the problem of bound-surface states,[9-11] surface-plasmon-assisted tunneling of electrons,[3] and the question of the additional boundary conditions (ABC) in semiconductor optics.[12]

If we look at the dispersion curves of surface polaritons in thin slabs, it will immediately be clear that retardation in the coupling of electrons to surface polaritons is only important at distances larger than c/ω_p. Thus it will depend on the specific nature of a given problem whether retardation is important or may be neglected. For instance, in bound-surface-state problems retardation is unimportant for deep states but will strongly change the wave function of shallow states, as in this case most of the wave function is in the retarded region of the potential. Following these arguments, the author has investigated the differential cross section for inelastic slow-electron scattering by surface-adsorbed dipoles.[13] Depending on the electron's energy and the scattering angles, retardation is shown to be more or less an important effect.

In this paper we derive the retarded coupling constants in close analogy to the nonretarded procedure.[1-5] Having performed the "retarded quantization," both the longitudinal and the transverse coupling Hamiltonians are derived in the polariton representation of a slab. In the next step the retarded single-loss spectrum is calculated and compared to the nonretarded one. Finally, the energy-resolved multiple-loss spectra are calculated by using the fast-particle approximation.[2] At the end we discuss how to include spatial dispersion effects and damping.

II. MODEL HAMILTONIAN

The dynamics of a dispersionless polarization field of a slab in contact with its own electromagnetic field can be derived from the following Hamiltonian:

$$H = \int d^3r \, \mathcal{H} , \tag{1a}$$

$$\mathcal{H} = 2\pi c^2 \vec{\Pi}^2 + \frac{1}{8\pi}(\vec{\nabla}\times\vec{A})^2 - \frac{1}{8\pi}(\vec{\nabla}\varphi)^2 - \varphi\vec{\nabla}\cdot\vec{P} + \left[\tfrac{1}{2}\omega_0^2 f\left(\vec{B} - \frac{1}{c}\vec{A}\right)^2 + \frac{1}{2f}\vec{P}^2\right]\Theta(a+z)\Theta(a-z) . \tag{1b}$$

The canonical variables describing the radiation field are the vector potential $\vec{A}$ and its canonically conjugate momentum $\vec{\Pi}$. Using the transverse gauge they obey the commutation relations[14]

$$[A_i(\vec{r}), \Pi_j(\vec{r}')] = i\hbar\delta_{ij}\delta(\vec{r}-\vec{r}') - i\hbar\frac{1}{4\pi}\frac{\partial}{\partial x_i}\frac{\partial}{\partial x_j'}\frac{1}{|\vec{r}-\vec{r}'|} . \tag{2}$$

The polarization field is described by the canonical pair of variables $\vec{P}$ and $\vec{B}$. They fulfill the commutation relations[15]

$$[P_i(\vec{r}), B_j(\vec{r}')] = \begin{cases} i\hbar\delta_{ij}\delta(\vec{r}-\vec{r}'), & -a \leq z, z' \leq +a \\ 0 \text{ elsewhere} . \end{cases} \tag{3}$$

The scalar potential φ (not being a canonical variable) is determined by the subsidiary condition

$$\Delta\varphi = 4\pi\vec{\nabla}\cdot\vec{P} , \tag{4}$$

and the constitutive relation folowing already from the classical equations of motions is given as

$$\epsilon(\omega)=1+\frac{4\pi f\omega_0^2}{\omega_0^2-\omega^2}. \tag{5}$$

In Eq. (5) ω_0 is the eigenfrequency due to short-range forces. In the case of a metal $\omega_0=0$, and $4\pi f\omega_0^2=\omega_p^2=4\pi ne^2/m$, with n being the density of electrons.

Polaritons are now defined in the usual way as solutions of Heisenberg's equation of motion:

$$i\hbar\dot{S}^+=[S^+,H]=-\hbar\omega_{\rm pol}S^+. \tag{6}$$

The generalized polariton operator S^+ is defined by a linear superposition of all the canonical fields appearing in the Hamiltonian density (1b):

$$S^+=\int d^3r[\vec{\alpha}(\vec{r})\cdot\vec{A}(\vec{r})+\vec{p}(\vec{r})\cdot\vec{\Pi}(\vec{r}) +\vec{\gamma}(\vec{r})\cdot\vec{P}(\vec{r})+\vec{\delta}(\vec{r})\cdot\vec{B}(\vec{r})]. \tag{7}$$

Next we insert the defining equation (7) in the equation of motion (6) and commute the resulting equation twice with each of the field operators A_i, Π_i, P_i, and B_i. Having performed all the commutations we arrive at the following coupled set of scalar equations of motion:

$$\frac{1}{4\pi}\Delta\vec{p}(\vec{r})-\frac{\omega_0^2 f}{c}\vec{\gamma}_t(\vec{r})-\frac{\omega_0^2 f}{c^2}\vec{p}_t(\vec{r})=i\omega_{\rm pol}\vec{\alpha}(\vec{r}), \tag{8a}$$

$$4\pi c^2\vec{\alpha}(\vec{r})=i\omega_{\rm pol}\vec{p}(\vec{r}), \tag{8b}$$

$$-\frac{1}{f}\vec{\delta}(\vec{r})+\vec{\nabla}_{\vec{r}}\int d^3r'\frac{\vec{\nabla}_{\vec{r}'}\cdot\vec{\delta}(\vec{r}')}{|\vec{r}-\vec{r}'|}=i\omega_{\rm pol}\vec{\gamma}(\vec{r}), \tag{8c}$$

$$\frac{\omega_0^2 f}{c}\vec{p}(\vec{r})+\omega_0^2 f\vec{\gamma}(\vec{r})=i\omega_{\rm pol}\vec{\delta}(\vec{r}). \tag{8d}$$

In Eq. (8a) the transverse-vector fields $\vec{\gamma}_t$ and $\vec{p}_t$ are defined by

$$\vec{\gamma}_t(\vec{r})=\vec{\gamma}(\vec{r})+\vec{\nabla}_{\vec{r}}\frac{1}{4\pi}\int d^3r'\frac{\vec{\nabla}_{\vec{r}'}\cdot\vec{\gamma}(\vec{r}')}{|\vec{r}-\vec{r}'|}, \tag{9}$$

$$\vec{p}_t(\vec{r})=\Theta(a+z)\Theta(a-z)\vec{p}(\vec{r}) +\vec{\nabla}_{\vec{r}}\frac{1}{4\pi}\int d^3r'\frac{\vec{\nabla}_{\vec{r}}\cdot\Theta(a+z')\Theta(a-z')\vec{p}(\vec{r}')}{|\vec{r}-\vec{r}'|}. \tag{10}$$

The appearance of these two transverse fields in Eq. (8a) is a consequence of using the transverse gauge in the canonical formulation of our problem.[16]

The solution of Eqs. (8a)–(8d) is performed in exactly the same manner as in the classical (nonquantized) case. There are three different types of coupled modes, and they are considered separately.

A. *s* waves

Since s waves are the *transverse* solutions of Eqs. (8), the vectors $\vec{\gamma}_t$ and γ are identical in this case. Thus following equation for $\vec{\alpha}$ is easily derived:

$$\Delta\vec{\alpha}(\vec{r})+\frac{\omega_{\rm pol}^2}{c^2}\vec{\alpha}(\vec{r})=-\Theta(a+z)\Theta(a-z)\frac{4\pi f\omega_0^2\omega^2}{(\omega_0^2-\omega^2)c^2}\vec{\alpha}(\vec{r}). \tag{11}$$

Once $\vec{\alpha}(\vec{r})$ is known, the other fields are derived:

$$\vec{p}(\vec{r})=-i\frac{4\pi c^2}{\omega_{\rm pol}}\vec{\alpha}(\vec{r}), \tag{12}$$

$$\vec{\gamma}(\vec{r})=+i\frac{4\pi c}{\omega_{\rm pol}}\frac{\omega_0^2}{\omega_0^2-\omega_{\rm pol}^2}\vec{\alpha}(\vec{r}), \tag{13}$$

$$\vec{\delta}(\vec{r})=c\frac{4\pi f\omega_0^2}{\omega_0^2-\omega_{\rm pol}^2}\vec{\alpha}(\vec{r}). \tag{14}$$

B. *p* waves

p waves are by definition the mixed modes of a slab. After lengthy but elementary calculations the following equation for $\vec{\delta}(\vec{r})$ is derived:

$$\Delta\vec{\delta}(\vec{r})+\frac{\omega_{\rm pol}^2}{c^2}\left(1+\frac{4\pi f\omega_0^2}{\omega_0^2-\omega_{\rm pol}^2}\right)\vec{\delta}(\vec{r})=0, \quad |z|\le a. \tag{15}$$

Once $\vec{\delta}$ is known the field $\vec{p}(\vec{r})$ is given as

$$\begin{aligned} i\frac{\omega_{\rm pol}}{c}\vec{p}(\vec{r})&=\frac{\omega_0^2-\omega_{\rm pol}^2}{f\omega_0^2}\vec{\delta}(\vec{r})-\vec{\nabla}_{\vec{r}}\int d^3r'\frac{\vec{\nabla}_{\vec{r}'}\cdot\vec{\delta}(\vec{r}')}{|\vec{r}-\vec{r}'|}, \quad |z|<a \\ i\frac{\omega_{\rm pol}}{c}\vec{p}(\vec{r})&=i\frac{\omega_{\rm pol}}{c}\vec{p}_{\rm homogen}-\vec{\nabla}_{\vec{r}}\int d^3r'\frac{\vec{\nabla}_{\vec{r}'}\cdot\vec{\delta}(\vec{r}')}{|\vec{r}-\vec{r}'|}, \quad |z|>a. \end{aligned} \tag{16}$$

In (15) $\vec{p}_{\rm homogen}$ is a solution of the homogeneous equation

$$\Delta\vec{p}_{\rm homogen}=\frac{\omega_{\rm pol}^2}{c^2}\vec{p}_{\rm homogen}. \tag{17}$$

The field $\vec{\alpha}$ follows from $\vec{p}$ by Eq. (8b), and the field $\vec{\gamma}$ is given with help of Eq. (8c).

C. Longitudinal solutions

In this case the transverse fields $\vec{\alpha}$ and $\vec{p}$ vanish, and the remaining fields $\vec{\gamma},\vec{\delta}$ are obtained by combining Eqs. (8c) and (8d) with $\vec{p}=\vec{0}$. The resulting longitudinal equation is well known and not reproduced here.

D. The boundary condition

We now want to discuss the boundary conditions under which Eqs. (11) and (15) and the longitudinal equation are to be solved. The operators representing the electric field strength $\vec{E}(\vec{r})$ and the magnetic field strength $\vec{H}(\vec{r})$ are expressed by the canonical fields in the usual way[14,16]:

$$\begin{aligned} \vec{E}(\vec{r})&=-4\pi c\vec{\Pi}(\vec{r})-\vec{\nabla}\varphi(\vec{r}) \\ &=-4\pi c\vec{\Pi}(\vec{r})+\vec{\nabla}_{\vec{r}}\int d^3r'\frac{\vec{\nabla}_{\vec{r}'}\cdot\vec{P}(\vec{r}')}{|\vec{r}-\vec{r}'|}, \end{aligned} \tag{18}$$

$$\vec{H}(\vec{r})=\vec{\nabla}\times\vec{A}(\vec{r}).$$

We imagine the slab to be slowly excited by just one polariton. To be specific, we consider a p polariton in what follows. The wave function in this case reads

$$|\,\rangle = c_0|\,0\rangle + c_i S_i^+|\,0\rangle\,, \tag{19}$$

where $|\,0\rangle$ is the vacuum (no polariton excited) and i is a quantum number. The expectation values of the electric and magnetic field, respectively, in the excited state (19) can be shown to be

$$\langle|\vec{\mathrm{E}}(\vec{\mathrm{r}})|\rangle = c_0 c_i^* \left(-\frac{\hbar\omega_{\mathrm{pol}}}{c}\vec{\mathrm{p}}_i^*(\vec{\mathrm{r}}) - i\hbar\vec{\nabla}_{\vec{\mathrm{r}}}\int d^3r'\,\frac{\vec{\nabla}_{\vec{\mathrm{r}}'}\cdot\vec{\delta}_i^*(\vec{\mathrm{r}}')}{|\vec{\mathrm{r}}-\vec{\mathrm{r}}'|}\right) + \mathrm{c.c.}, \tag{20}$$

$$\langle|\vec{\mathrm{H}}(\vec{\mathrm{r}})|\rangle = -c_0 c_i^* i\hbar\vec{\nabla}_{\vec{\mathrm{r}}}\times\vec{\mathrm{p}}_i^*(\vec{\mathrm{r}}) + \mathrm{c.c.} \tag{21}$$

Since Maxwell's equations persist in their operator form,[14,16] the Maxwell boundary conditions are derived for the corresponding expectation values. Thus we arrive at the following boundary conditions (for p waves):

$$\frac{\omega_0^2-\omega_i^2}{f\omega_0^2}\vec{\delta}_i^t(\vec{\mathrm{r}})\Big|_{z=\pm a} = \frac{i\omega_i}{c}\vec{\mathrm{p}}_{i,\mathrm{homogen}}^t(\vec{\mathrm{r}})\Big|_{z=\pm a}, \tag{22}$$

$$\frac{\omega_0^2-\omega_i^2}{f\omega_0^2}[\vec{\nabla}_{\vec{\mathrm{r}}}\times\vec{\delta}_i(\vec{\mathrm{r}})]^t\Big|_{z=\pm a} = \frac{i\omega_i}{c}[\vec{\nabla}_{\vec{\mathrm{r}}}\times\vec{\mathrm{p}}_{i,\mathrm{homogen}}(\vec{\mathrm{r}})]^t\Big|_{z=\pm a}. \tag{23}$$

After identifying $\vec{\delta}$ with the classical polarization $\vec{\mathrm{P}}_{\mathrm{class}}$, and the field $\vec{\mathrm{p}}$ with the classical vector potential $\vec{\mathrm{A}}_{\mathrm{class}}$, the boundary conditions (22) and (23) are seen to agree with the classical boundary conditions for p waves.[17,18] The same analysis holds for s waves and for the longitudinal modes.

Owing to the same boundary conditions, the classical eigenvalue equations are reproduced.[17,18] Thus we are left to determine the polariton norming constants.

E. The polariton norming constants

The correct polariton normalization is demonstrated in the following for s waves as an example. Due to the homogeneous nature of the Eqs. (8a)–(8d), there is only one free constant which must be determined to yield

$$[S_i, S_j^+] = \delta_{ij}\,. \tag{24}$$

Since we start with the field $\vec{\alpha}$, the free constant is contained in this field. Using the Eqs. (11)–(14), the polariton commutator (24) between s waves is derived to be

$$[S_i, S_j^+] = 4\pi\hbar c^2\left(\frac{1}{\omega_i}+\frac{1}{\omega_j}\right) \times\int d^3r\,\vec{\alpha}_i^*\cdot\vec{\alpha}_j\left(1+\frac{4\pi f\omega_0^2}{\omega_0^2-\omega_i^2}\frac{\omega_0^2}{\omega_0^2-\omega_j^2}\times\Theta(a+z)\Theta(a-z)\right). \tag{25}$$

The orthogonality for $i\neq j$ is easily shown by using Eq. (11) for two different eigenvalues:

$$-\Delta\vec{\alpha}_i(\vec{\mathrm{r}}) + V(z;\lambda_i)\vec{\alpha}_i(\vec{\mathrm{r}}) = \lambda_i\vec{\alpha}_i(\vec{\mathrm{r}})\,, \tag{26a}$$

$$-\Delta\alpha_j^*(\vec{\mathrm{r}}) + V(z;\lambda_j)\vec{\alpha}_j^*(\vec{\mathrm{r}}) = \lambda_j\vec{\alpha}_j^*(\vec{\mathrm{r}})\,. \tag{26b}$$

In Eqs. (26a) and (26b) we have defined

$$\lambda_{i,j} = \frac{\omega_{i,j}^2}{c^2},\quad V(z;\lambda_{i,j}) = \Theta(a+z)\Theta(a-z)\lambda_{i,j}\frac{4\pi f\omega_0^2}{\omega_0^2-c^2\lambda_{i,j}^2}. \tag{27}$$

Multiplying Eq. (26a) with $\vec{\alpha}_j^*$ from the left and Eq. (26b) with $\vec{\alpha}_i$ from the right, and integrating

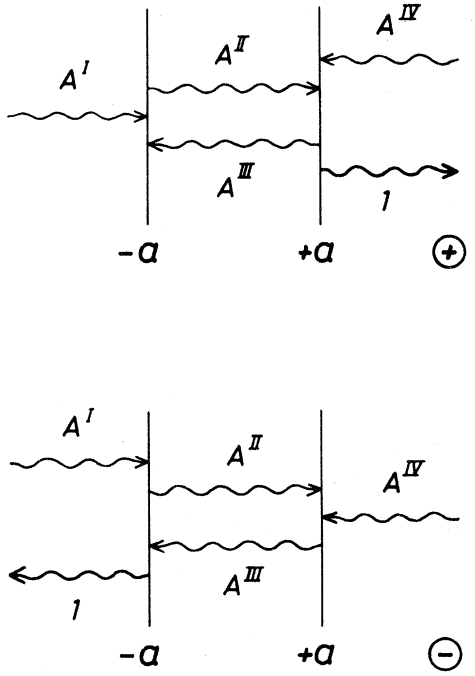

FIG. 1. Polariton states in this paper are defined as usual in any quantum-mechanical scattering problem. The figure shows the coupled scattering states of photons inside and outside the slab, respectively, and polarization quanta inside the slab (at normal incidence). Incoming boundary conditions have been chosen. The amplitudes A^{I}–A^{IV} agree with the classical ones. To obtain the correct quantum-mechanical polariton normalization, all the numbers $(1, A^{\mathrm{I}}$–$A^{\mathrm{IV}})$ must be multiplied with the factor C given in Eq. (34) of the text.

over the coordinate $\vec{r}$, the orthogonality is immediately clear.

Next we determine the polariton norming constant. To this end we have to distinguish between the nonradiative modes and the radiative ones.[17,18] The nonradiative modes follow from

$$\vec{\alpha}(\vec{r}) \equiv \vec{\alpha}_{\vec{q},\pm,i}(\vec{r}) = \frac{e^{i\vec{q}\cdot\vec{\rho}}}{2\pi} A_{q,\pm,i}(z)\vec{e}_z \times \frac{\vec{q}}{q} \tag{28}$$

with

$$A_{q,+,i}(z) = C_{q,+,i} * \begin{cases} e^{\alpha_{q,+,i}a}\cos(\beta_{q,+,i}a)e^{\alpha_{q,+,i}z}, & z < -a \\ \cos(\beta_{q,+,i}z), & |z| < a \\ e^{\alpha_{q,+,i}a}\cos(\beta_{q,+,i}a)e^{-\alpha_{q,+,i}z}, & z > +a \end{cases} \tag{29}$$

and

$$A_{q,-,i}(z) = C_{q,-,i} * \begin{cases} -e^{\alpha_{q,-,i}a}\sin(\beta_{q,-,i}a)e^{\alpha_{q,-,i}z}, & z < -a \\ \sin(\beta_{q,-,i}z), & |z| < a \\ e^{\alpha_{q,-,i}a}\sin(\beta_{q,-,i}a)e^{-\alpha_{q,-,i}z}, & z > +a. \end{cases} \tag{30}$$

The propagation constants $\alpha_{q,\pm,i}$ and $\beta_{q,\pm,i}$ are defined as known from the nonquantized case:

$$\begin{aligned} \alpha_{q,\pm,i} &= [q^2 - \omega_{\pm,i}^2(q)/c^2]^{1/2}, \\ \beta_{q,\pm,i} &= [q^2 - \omega_{\pm,i}^2(q)\epsilon(\omega_\pm(q))/c^2]^{1/2}, \end{aligned} \tag{31}$$

and the frequencies $\omega_{\pm,i}(q)$ follow from the classical eigenvalue equations.[17] Using (29) and (30), the norming constants are derived as follows:

$$|C_{q,+,i}|^{-2} = \frac{8\pi\hbar c^2 a}{\omega_{+,i}(q)}\left[\frac{\cos^2(\beta_{q,+,i}a)}{\alpha_{q,+,i}a} + \frac{1}{4\pi f}[\epsilon(\omega_{+,i}(q)) - 1]^2\left(1 + \frac{\sin(2\beta_{q,+,i}a)}{2\beta_{q,+,i}a}\right)\right], \tag{32a}$$

$$|C_{q,-,i}|^{-2} = \frac{8\pi\hbar c^2 a}{\omega_{-,i}(q)}\left[\frac{\sin^2(\beta_{q,-,i}a)}{\alpha_{q,-,i}a} + \frac{1}{4\pi f}[\epsilon(\omega_{-,i}(q)) - 1]^2\left(1 - \frac{\sin(2\beta_{q,-,i}a)}{2\beta_{q,-,i}a}\right)\right]. \tag{32b}$$

In the radiative region of the dispersion plane[17,18] ($q < \omega/c$) the eigenvalues of a given q are continuous. So we introduce scattering wave functions with *incoming scattered waves* far away from the slab (see Fig. 1). Owing to the same boundary conditions at the slab surfaces $\pm a$, the constants $A_{+,-}^{\mathrm{I,II,III,IV}}$ agree with the classical ones. If we use the frequency itself as third quantum number in the continuum

$$[S_{\vec{q},\omega}, S^+_{\vec{q}',\omega'}] = \delta(\vec{q} - \vec{q}')\delta(\omega - \omega'), \tag{33}$$

the additional constant multiplying all the "classical constants" is given as

$$C = \frac{\omega}{4\pi c^2}[\hbar\tilde{\alpha}(q,\omega)]^{-1/2}, \quad \tilde{\alpha}(q,\omega) = (\omega^2/c^2 - q^2)^{1/2}. \tag{34}$$

The same procedure applied to the p waves is much more elaborate. Thus we give only some results which are central to the electron–surface-polariton scattering. The general polariton commutator within two different p-wave states can be calculated by using the wave functions of Sec. II B with the following result (i,j in the following is short for all the quantum numbers being relevant):

$$[S_i, S_j^+] = \frac{\hbar}{4\pi c^2}(\omega_i + \omega_j)\langle\vec{p}_i \,|\, \vec{p}_j\rangle_{\text{all space}} + \frac{\hbar}{\omega_0^2 f}(\omega_i + \omega_j)\langle\vec{\delta}_i \,|\, \vec{\delta}_j\rangle_{\text{slab}} + \frac{i\hbar}{c}(\langle\langle\vec{\delta}_i \,|\, \vec{p}_j\rangle_{\text{slab}} - \langle\vec{p}_i \,|\, \vec{\delta}_j\rangle_{\text{slab}}) \stackrel{!}{=} \delta(i-j). \tag{35}$$

If we write the $\vec{B}$ part of the surface-polariton creation operator [solution of Eq. (15)] in the form

$$\vec{\delta}_{s,\vec{q},-}(\vec{r}) = C_{s,q,-}\frac{e^{i\vec{q}\cdot\vec{\rho}}}{2\pi}\left(\frac{\vec{q}}{q}\cosh(\beta_{s,q,-}z) - \vec{e}_z i\frac{q}{\beta_{s,q,-}}\sinh(\beta_{s,q,-}z)\right), \tag{36}$$

$$\vec{\delta}_{s,\vec{q},+}(\vec{r}) = C_{s,q,+}\frac{e^{i\vec{q}\cdot\vec{\rho}}}{2\pi}\left(\frac{\vec{q}}{q}\sinh(\beta_{s,q,+}z) - \vec{e}_z i\frac{q}{\beta_{s,q,+}}\cosh(\beta_{s,q,+}z)\right), \tag{37}$$

with $\beta_{s,q,\pm}$ following from (31) by replacing the index i by s, and with $\omega_{\pm,s}(q)$ following from the well known equation

$$\left(\frac{q^2 - \omega^2\epsilon(\omega)/c^2}{q^2 - \omega^2/c^2}\right)^{1/2}\tanh[a(q^2 - \omega^2\epsilon(\omega)/c^2)^{1/2}] = -\epsilon(\omega) \text{ for } \omega_+, \tag{38}$$

$$\left(\frac{q^2 - \omega^2\epsilon(\omega)/c^2}{q^2 - \omega^2/c^2}\right)^{1/2}\coth[a(q^2 - \omega^2\epsilon(\omega)/c^2)^{1/2}] = -\epsilon(\omega) \text{ for } \omega_- \tag{39}$$

We need to calculate the constants $C_{s,q,\pm}$. After very lengthy but elementary calculations they are determined to be

$$|C_{s,\pm,q}|^{-2}=\left[\frac{8\pi\hbar/\omega_{s,\pm}}{(\epsilon_\pm-1)^2}+\frac{8\pi\hbar\omega_{s,\pm}}{4\pi\omega_0^2 f}\left(1+\frac{4\pi\omega_0^2 f/\omega_{s,\pm}^2}{\epsilon_\pm-1}\right)\right]a\left(\frac{q^2+\beta_\pm^2}{\beta_\pm^2}\frac{\sinh(2a\beta_\pm)}{2\beta_\pm a}\mp\frac{\beta_\pm^2-q^2}{\beta_\pm^2}\right)$$
$$+\frac{\hbar 32\pi q e^{-qa}\epsilon_\pm}{\omega_{s,\pm}\beta_\pm^2(\epsilon_\pm-1)}\times\begin{Bmatrix}\cosh^2(\beta_+a)\sinh(qa)\\ \sinh^2(\beta_-a)\cosh(qa)\end{Bmatrix}+\frac{\hbar 16\pi(q^2+\alpha_\pm^2)}{\omega_{s,\pm}(\epsilon_\pm-1)^2\alpha_\pm^3}\times\begin{Bmatrix}\sinh^2(\beta_+a)\\ \cosh^2(\beta_-a)\end{Bmatrix}$$
$$+\frac{\hbar 16\pi q e^{-qa}\sinh(2\beta_\pm a)}{\omega_{s,\pm}(\epsilon_\pm-1)\beta_\pm\alpha_\pm}\times\begin{Bmatrix}\sinh(qa)\\ \cosh(qa)\end{Bmatrix}. \tag{40}$$

In (40) β_+, etc., is short for $\beta_{s,q,+}$, etc.

F. Fields in the slab-polariton representation

Since the orthonormalized solutions of the Eqs. (8) provide a complete set of states the field operators $\vec{A}(\vec{r})$, $\vec{\Pi}(\vec{r})$, $\vec{P}(\vec{r})$, and $\vec{B}(\vec{r})$ are given in turn as a linear superposition of all the polariton creation and annihilation operators. The derivation proceeds in close analogy to the infinite crystal (or vacuum) case and is not given here. In what follows, we quote the results only in a somewhat implicit form, because the explicit writing of all the formulas is not very illuminating and can be obtained from the author at request. It is only the longitudinal part of $\vec{P}$ that is given explicitly, since the normalization that we have used differs from that given in the literature.[2] Of course, the physics is the same. We have

$$\vec{P}(\vec{r})=\vec{P}_l(\vec{r})+\vec{P}_s(\vec{r})+\vec{P}_p(\vec{r}), \tag{41}$$

$$\vec{P}_l(\vec{r})=\sum_i\frac{\hbar\omega_0^2 f}{\omega_l}[\vec{\gamma}_{l,i}(\vec{r})S_{l,i}+\text{H.c.}], \tag{42}$$

$$\vec{\gamma}_{l,i}(\vec{r})\equiv\vec{\gamma}_{l,\vec{q},\pm,m}(\vec{r}), \tag{43}$$

$$\vec{\gamma}_{l,\vec{q},+,m}(\vec{r})=C_{l,q,+,m}\frac{e^{i\vec{q}\cdot\vec{\rho}}}{2\pi}\times\left[\vec{q}i\sin\left(\frac{m\pi z}{2a}\right)+\vec{e}_z\frac{m\pi}{2a}\cos\left(\frac{m\pi z}{2a}\right)\right], \tag{44}$$
$$m=2,4,6,\ldots$$

$$\vec{\gamma}_{l,\vec{q},-,m}(\vec{r})=C_{l,\vec{q},-,m}\frac{e^{i\vec{q}\cdot\vec{\rho}}}{2\pi}\times\left[\vec{q}i\cos\left(\frac{m\pi z}{2a}\right)-\vec{e}_z\frac{m\pi}{2a}\sin\left(\frac{m\pi z}{2a}\right)\right], \tag{45}$$
$$m=1,3,5,\ldots$$

$$C_{l,q\pm,m}=\left(\frac{\omega_l}{2\hbar\omega_0^2 fa[q^2+m^2\pi^2/(4a^2)]}\right)^{1/2}, \tag{46}$$

$$\vec{P}_s(\vec{r})=\sum_i\left(i\hbar c\frac{4\pi f\omega_0^2}{\omega_0^2-\omega_i^2}\vec{\alpha}_{s,i}(\vec{r})S_{s,i}+\text{H.c.}\right), \tag{47}$$

$$\vec{P}_p(\vec{r})=\sum_i[i\hbar c\vec{\delta}_{p,i}(\vec{r})S_{p,i}+\text{H.c.}], \tag{48}$$

$$\vec{B}(\vec{r})=\vec{B}_l(\vec{r})+\vec{B}_s(\vec{r})+\vec{B}_p(\vec{r}), \tag{49}$$

$$\vec{B}_l(\vec{r})=\sum_i[i\hbar\vec{\gamma}^*_{l,i}(\vec{r})S^+_{l,i}+\text{H.c.}], \tag{50}$$

$$\vec{B}_s(\vec{r})=\sum_i\left(\frac{4\pi\hbar c\omega_0^2}{\omega_{s,i}(\omega_0^2-\omega_{s,i}^2)}\vec{\alpha}_{s,i}(\vec{r})S_{s,i}+\text{H.c.}\right), \tag{51}$$

$$\vec{B}_p(\vec{r})=\sum_i\left[\left(\frac{\hbar\omega_{p,i}}{\omega_0^2 f}\vec{\delta}_{p,i}(\vec{r})+\frac{i\hbar}{c}\vec{p}_{p,i}(\vec{r})\right)S_{p,i}+\text{H.c.}\right], \tag{52}$$

$$\vec{A}(\vec{r})=\vec{A}_s(\vec{r})+\vec{A}_p(\vec{r}), \tag{53}$$

$$\vec{A}_s(\vec{r})=\sum_i\left(\frac{4\pi\hbar c^2}{\omega_{s,i}}\vec{\alpha}_{s,i}(\vec{r})S_{s,i}+\text{H.c.}\right), \tag{54}$$

$$\vec{A}_p(\vec{r})=\sum_i[i\hbar\vec{p}_{p,i}(\vec{r})S_{p,i}+\text{H.c.}], \tag{55}$$

$$\vec{\Pi}(\vec{r})=\vec{\Pi}_s(\vec{r})+\vec{\Pi}_p(\vec{r}), \tag{56}$$

$$\vec{\Pi}_s(\vec{r})=\sum_i[i\hbar\vec{\alpha}_{s,i}(\vec{r})S_{s,i}+\text{H.c.}], \tag{57}$$

$$\vec{\Pi}_p(\vec{r})=\sum_i\left(\frac{\hbar\omega_{p,i}}{4\pi c^2}\vec{p}_{p,i}(\vec{r})S_{p,i}+\text{H.c.}\right). \tag{58}$$

We are now in a position to derive the slab-polariton representation of any interaction Hamiltonian describing the coupling of an external source to the slab. This is performed in the next section for the complete retarded electron–surface-polariton coupling.

III. RETARDED ELECTRON-SURFACE-POLARITON COUPLING

An "external" electron couples to the eigenmodes of a slab by the longitudinal charge-density coupling and via the transverse-photon exchange coupling. Thus retardation comes into play by two rather different effects.

First, the nonretarded longitudinal charge-density coupling will be changed by retardation due to the retarded nature of the *true* eigenmodes of a slab. This results in a drastic change of the electron-to-surface-mode coupling at $\vec{q}$ values being smaller than ω_l/c. In addition, the *true* volume p waves couple by their surface charge density to the electron. This latter type of coupling is missing in the so-called nonretarded limit.

Second, in addition to the nonretarded charge-density coupling we have to take into account the retarded photon exchange coupling. It vanishes in the limit $c\to\infty$.

A. Longitudinal charge-density coupling

The coupling Hamiltonian is simply given by the Coulomb interaction of the external electron to the polarization charge density of the slab. Thus we write

$$H_l' = \int\int d^3r\, d^3r' \frac{\rho_e(\vec{r})\rho_{\rm pol}(\vec{r}')}{|\vec{r}-\vec{r}'|} \tag{59}$$

with

$$\rho_e(\vec{r}) = -e\rho(\vec{r}-\vec{r}_e) \tag{60}$$

and

$$\rho_{\rm pol}(\vec{r}') = -\vec{\nabla}_{\vec{r}'}\cdot\vec{P}(\vec{r}')\,. \tag{61}$$

The polarization charge density contains the purely longitudinal volume part, the volume part of the p waves, and the surface part of these modes. So, this operator can be split further as follows:

$$\vec{\nabla}_{\vec{r}'}\cdot\vec{P}(\vec{r}') = \vec{\nabla}\cdot\vec{P}_l + \vec{\nabla}\cdot\vec{P}_p^{\rm volume} + \vec{\nabla}\cdot\vec{P}_p^{\rm surface}\,. \tag{62}$$

It is the last part of (62) which is central to the present paper. The second part of (62) contributes to the quantized analog of the transition and Čerenkov radiation *and* to the volume part of the image potential. The first part has been dealt with extensively in the literature[2] and is only considered at the end, where some numerical examples are given.

The evaluation of the part of the integral (59) following from the third part of (62) runs through as known from the nonretarded version of this operator.[2] So, we give only the result without any derivation:

$$H_{l,\rm surface}' = \sum_{+,-} -e\hbar \int\int d^2\vec{q}\, C_{s,q,\pm}\frac{e^{i\vec{q}\cdot\vec{r}_e}}{\beta_{s,q,\pm}}\times\begin{Bmatrix}\cosh(a\beta_{s,q,+})\\ \sinh(a\beta_{s,q,-})\end{Bmatrix}(e^{-q|z_e-a|}\mp e^{-q|z_e+a|})(S_{s,\vec{q},\pm}+S^+_{s,\vec{q},\pm})\,. \tag{63}$$

In (63) the norming constants $C_{s,q,\pm}$ are given by (40) and the retarded propagation constants $\beta_{s,q,\pm}$ are explained in context with Eqs. (36) and (37).

If we want to go back to the nonretarded coupling Hamiltonian, we simply replace $\beta_{s,q,\pm}$ by q and the retarded norming constants by their nonretarded expression

$$|C^{\rm nonretarded}_{s,q,\pm}|^{-2} = \frac{8\pi\hbar\omega^{\rm nonretarded}_{s,q,\pm}\sinh(2qa)}{4\pi\omega_0^2 fq}\,. \tag{64}$$

B. Transverse-photon exchange coupling

In contrast to the charge-density coupling, the transverse coupling itself is a retarded one and vanishes for $c\to\infty$. It is only important at higher velocities of the scattered electron. Thus, we give numerical results only at high electron velocities. The volume part of this coupling term is deferred to another paper, where all the retarded volume parts are considered on the same footing.

In a fully-quantum-mechanical description of the electron-slab problem the coupling Hamiltonian in question can be derived from the electron part of the total Hamiltonian in the presence of a vector potential $\vec{A}(\vec{r})$:

$$H_{e-\vec{A}} = \frac{1}{2m}\left(\frac{\hbar}{i}\vec{\nabla}_{\vec{r}_e} + \frac{e}{c}\vec{A}(\vec{r}_e)\right)^2. \tag{65}$$

Next we write $\vec{A}$ as given in (53) and arrive at the slab polariton representation of the coupling by using (54) and (55).

In fast-electron spectroscopy this quantization scheme is actually superfluous. In fact, the fast-particle approximation can be used,[19] regarding the electron as a source for energy and momentum. Thus the external electron couples to the normal modes of a slab by its scalar Coulomb potential, Eq. (59) in the fast-particle approximation, and by its vector potential $\vec{A}_{\rm ext}(\vec{r};\vec{v}_e,\vec{r}_e)$. The slab couples to this external vector potential by the polarization current density.[20] We end with

$$H_t' = -\frac{\omega_0^2 f}{c}\int\int\frac{d^2q}{4\pi^2}\int\int d^2\rho\left(\vec{B}(\vec{r})-\frac{1}{c}\vec{A}(\vec{r})\right)\cdot\vec{A}_{\rm ext}(\vec{q},z;\vec{v},\vec{r}_e)e^{i\vec{q}\cdot\vec{\rho}}\,. \tag{66}$$

The surface part of the current-density operator follows from Eqs. (52) and (55). The $-\vec{q}$ component of this operator is given as

$$\vec{B}(-\vec{q},z) - \frac{1}{c}\vec{A}(-\vec{q},z) = \sum_{+,-}\frac{\hbar\omega_{s,q,\pm}}{\omega_0 f}\vec{\delta}_{s,-\vec{q},\pm}(z)S_{s,-\vec{q},\pm} + \text{H.c.} \tag{67}$$

Finally, the transverse vector potential of a moving electron with a constant velocity $\vec{v}$ follows from Maxwell's equations:

$$\vec{A}_{\rm ext}(\vec{q}_\parallel, z, \vec{v}, \vec{r}_e) = -\frac{e4\pi c}{c^2 - v_z^2} e^{-i\vec{q}\cdot\vec{\rho}_e} * \int_{-\infty}^{+\infty} \frac{dq_z}{2\pi} \frac{e^{iq_z(z-z_e)}}{(q_z - q_z^1)(q_z - q_z^{1*})}\left(1 - \frac{(\vec{Q}\cdot\vec{v})\vec{Q}}{(q_z - q_z^2)(q_z - q_z^{2*})}\right),$$
$$\vec{Q} = (\vec{q}_\parallel, q_z). \tag{68}$$

In (68) the retarded and unretarded poles of the vector potential are defined as follows:

$$q_z^1 = (1 - v_z^2/c^2)^{-1}\left[v_z(\vec{q}_\parallel\cdot\vec{v})/c^2 + iq\left(1 - \frac{v_z^2 + (\vec{q}_\parallel\cdot\vec{v})^2/q^2}{c^2}\right)^{1/2}\right], \tag{69}$$

$$q_z^2 = iq, \tag{70}$$

and the asterisk in (68) means the conjugate complex. In the fast-particle approximation the electron coordinate is taken on its classical trajectory $\vec{r}_e = \vec{v}t = \vec{v}_\parallel t + \vec{v}_z t$.

IV. COUPLING INTEGRALS IN THE FAST-PARTICLE APPROXIMATION

For the purpose of calculating the energy-loss spectrum due to surface-polariton excitation we proceed in exactly the same manner as described in detail in the work by Šunjić and Lucas.[2] Therefore, we give only a short summary of their method.

The dynamics of the slab being coupled to the external electron by the interaction Hamiltonians (63) and (66) can exactly be solved. In the interaction picture the time evolution of the slab wave function is

$$|\psi^I(t)\rangle = \exp\left[-\frac{i}{\hbar}\left(\sum_\lambda J_\lambda(t, t_0)S_\lambda + \text{H.c.}\right)\right]|\psi^I(t_0)\rangle, \tag{71}$$

where $J_\lambda(t, t_0)$ is the time integral

$$J_\lambda(t, t_0) = \int_{t_0}^{t} dt' I_\lambda(t') e^{-i\omega_\lambda t'}, \tag{72}$$

and $I_\lambda(t')$ are the coupling integrals appearing in (63) and (66). λ is short for the quantum numbers in question.

The power spectrum is given by

$$P(\omega) = \lim_{\substack{t\to\infty \\ t_0\to-\infty}} \sum_{[\Lambda]} |\langle\psi^I(t, t_0)|[\Lambda]\rangle|^2 \delta(\omega - \omega_{[\Lambda]}), \tag{73}$$

where the sum runs over *all* possible many polariton states $[\Lambda]$. $P(\omega)$ is shown to be the Fourier transform of a time correlation function $P(t)$:

$$P(\omega) = \frac{1}{2\pi}\int_{-\infty}^{+\infty} dt\, e^{i\omega t} P(t), \tag{74}$$

$$P(t) = \langle 0|\, U^\dagger(t)U(0)|0\rangle, \tag{75}$$

$$U(t) = \exp\left[-\frac{i}{\hbar}\left(\sum_\lambda J_\lambda(+\infty, -\infty)S_\lambda e^{-i\omega_\lambda t} + \text{c.c.}\right)\right]. \tag{76}$$

$P(t)$ can be further reduced by using standard methods of evaluating expectation values like (75). The final result is quite simple:

$$P(t) = \exp\left(-\frac{1}{\hbar^2}\sum_\lambda |J_\lambda(+\infty, -\infty)|^2\right) \times \exp\left(\frac{1}{\hbar^2}\sum_\lambda |J_\lambda(+\infty, -\infty)|^2 e^{-i\omega_\lambda t}\right). \tag{77}$$

In this paper we study the surface part of the correlation function (77) in the power spectrum (74). In addition, all retarded results are compared to the nonretarded ones. Following Šunjić and Lucas we separate the dispersive part of the spectrum in writing (77) in the form

$$P(t) = \exp\left(-\frac{1}{\hbar^2}\sum_{+,-}\iint d^2q\,|J_{\pm,\vec{q}}(+\infty, -\infty)|^2\right)\exp\left(\frac{1}{\hbar^2}\sum_{+,-}\int_{q_{nd}}^{q_c} q\,dq\int_0^{2\pi} d\varphi\,|J_{\pm,q,\varphi}(+\infty, -\infty)|^2 e^{-i\omega_s t}\right)$$
$$\times\left[\exp\left(\frac{1}{\hbar^2}\sum_{+,-}\int_0^{q_{nd}} q\,dq\int_0^{2\pi} d\varphi\,|J_{\pm,q,\varphi}(+\infty, -\infty)|^2 e^{-i\omega_\pm(q)t}\right) - 1 + 1\right]. \tag{78}$$

The first exponential determines the strength of the no-surface-loss contribution to the no-loss line, the second exponential determines the strength of the nondispersive multiple surface-loss peaks at $n\omega_s$, where $\omega_s = \omega_1/\sqrt{2}$ in case of a metal, and the strength of the dispersive multiple losses is contained in the last exponential function minus one. The q integration for determining the dispersive part ends at q_{nd}, the end point of dispersion on the surface polariton curves. Beyond q_{nd} retardation may surely be neglected. Therefore, the integral in the second integral is the nonretarded one.[2] The integration ends at q_c, the critical wavelength beyond which the macroscopic model is ill defined.[2]

The "dispersive part" of the correlation function (78) creates two different effects. First, its Fourier transform

$$S_0(\omega) = \int_{-\infty}^{+\infty}\frac{dt}{2\pi}e^{i\omega t}\left[\exp\left(\frac{1}{\hbar^2}\sum_{+,-}\int_0^{q_{nd}} q\,dq\int_0^{2\pi} d\varphi\,|J_{\pm,q,\varphi}(+\infty, -\infty)|^2 e^{-i\omega_\pm(q)t}\right) - 1\right] \tag{79}$$

determines the pure dispersive part of the spectrum. Second, by replacing the frequency ω in (79), by $(\omega - n\omega_s)$ and multiplying the integral with P_n^s defined as

$$P_n^s = \frac{1}{n!}\left(\frac{1}{\hbar^2}\sum_{+,-}\int_{q_{nd}}^{q_c} q\,dq\int_0^{2\pi} d\varphi\,|J_{\pm,q,\varphi}(+\infty,-\infty)|^2\right)^n \tag{80}$$

we obtain the repetition of the dispersive part of the spectrum at each nondispersive multiple loss $n\omega_s$.

The key quantity determining the strength of the "multiple dispersive surface-polariton loss peaks" is the first-order analog to $S_0(\omega)$. It is obtained by expanding the exponential function in (79) up to first order:

$$S_0^1(\omega) = \frac{1}{\hbar^2}\sum_{+,-}\int_0^{q_{nd}} q\,dq\int_0^{2\pi} d\varphi|J_{\pm,q,\varphi}(+\infty,-\infty)|^2 \times\delta(\omega-\omega_\pm(q))$$

$$\equiv\frac{1}{\omega_l}\sum_{+,-}\int_0^{Q_{nd}} dQ\,X_\pm(Q)\delta(\Omega-\Omega_\pm(Q)). \tag{81}$$

In (81) Q and Ω are the reduced wave vector and frequency, respectively, defined by $Q=q/q_l$ and $\Omega=\omega/\omega_l$ where ω_l is, as before, the frequency of the longitudinal modes and $q_l=\omega_l/c$. The dimensionless *coupling integrals*

$$X_\pm(Q) = q_l^2 Q\int_0^{2\pi} d\varphi\,|J_{\pm,Q,\varphi}(+\infty,-\infty)|^2 \tag{82}$$

contain all the information we need. For instance, the first-order line shape is obtained by multiplying $X_\pm(Q)$ with $[d\Omega_\pm(Q)/dQ]^{-1}$ and summing up the integral at a given frequency. Another piece of information contained in the coupling integrals is the number of scattered electrons on an elliptic cone centered around the trajectory of the fast electron (see Fig. 2). In the next section the re-

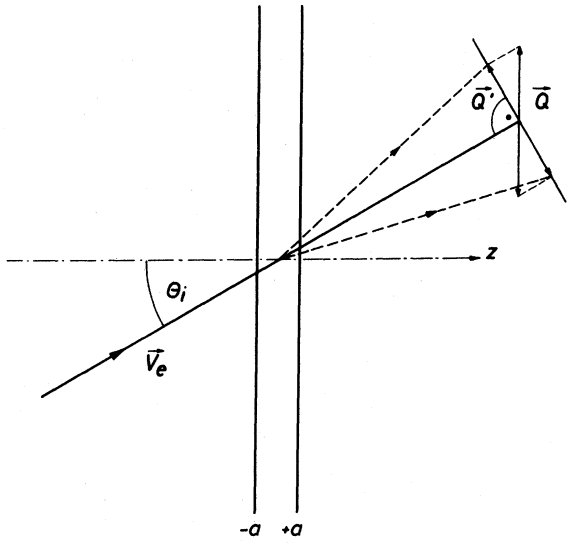

FIG. 2. The incoming electron of velocity $\vec{V}_e$ and angle of incidence θ_i will be scattered by surface polaritons. The coupling integrals as defined by Eqs. (81)–(83) in text give a clear picture of which part of the dispersion curve is effective in angular and energy spread of the incoming electron beam. As can be seen from Eq. (81) the coupling integrals are within the first-order theory a direct measure for the number of scattered electrons on an elliptic cone, being centered around $\vec{V}_e$.

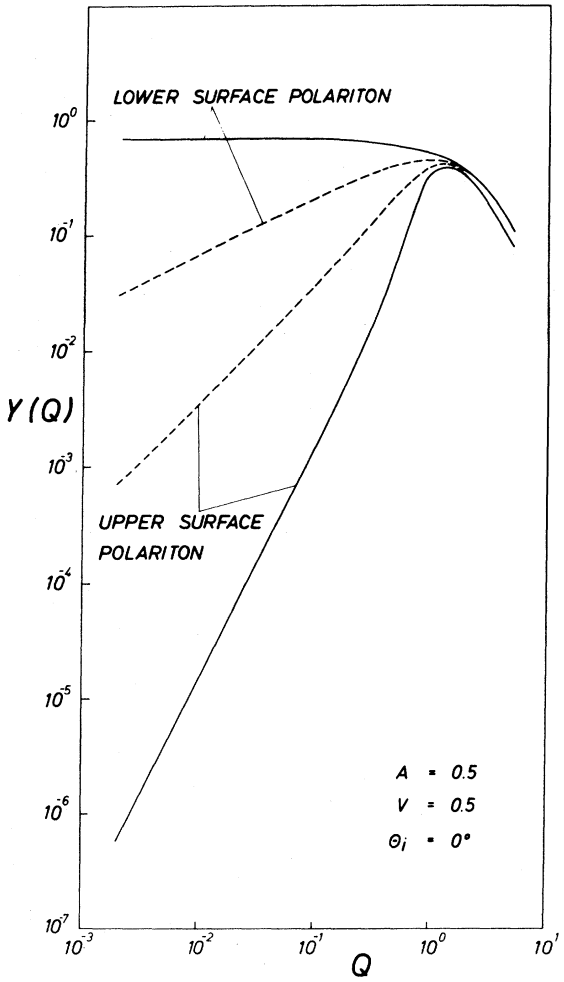

FIG. 3. Reduced dimensionless coupling integral $Y_\pm(Q)$ [see Eqs. (81)–(83) in the text] as a function of the dimensionless wave number $Q=q/q_l$ with $q_l=4\pi ne^2/mc$. The electron velocity is given in units of c, where c is the velocity of light in vacuum. A is a dimensionless thickness parameter defined as $q_l a$, where a is half of the slab thickness. θ_i is the angle of incidence, measured relative to the slab normal. Continuous line: scattering with inclusion of retardation; broken line: without retardation. To be short, the word polariton is used in the figures for both cases.

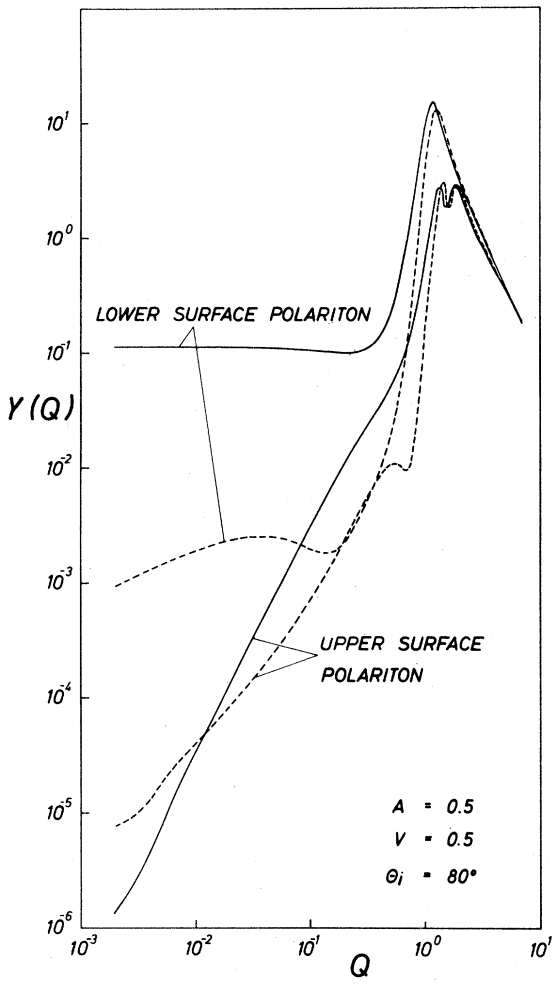

FIG. 4. The same as Fig. 3 but with another angle of incidence.

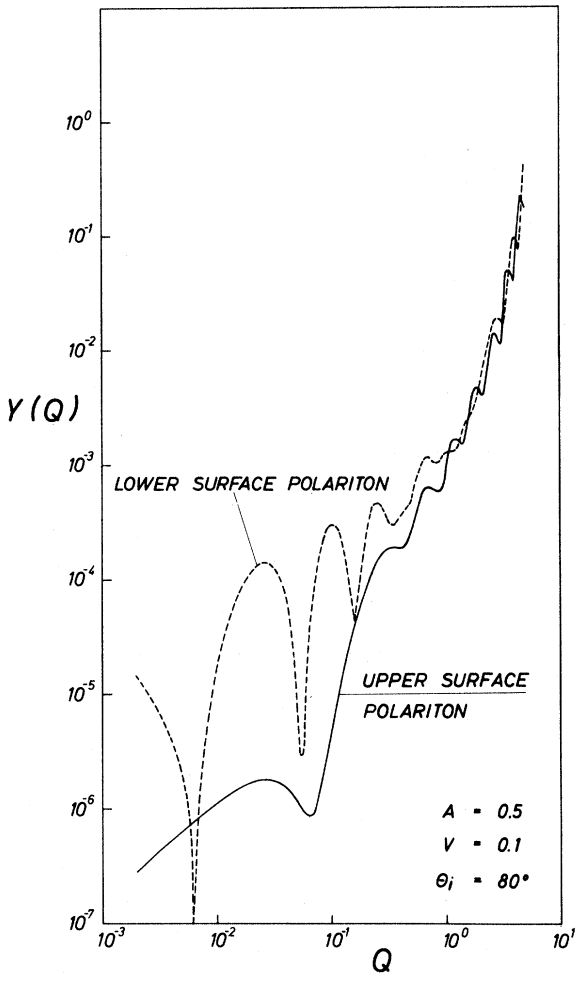

FIG. 5. Unretarded scattering in case of $A = 0.5$, $V = 0.1$, $\theta_i = 80°$ (for the meaning of symbols see text to Fig. 3). The pronounced oscillations in the scattering efficiency can be interpreted as "resonant" or "anti-resonant" coupling of fast electrons to surface excitations at a certain $\vec{q}$ vector.

tarded coupling integrals are discussed in some detail and compared to the nonretarded ones.

V. RESULTS AND DISCUSSION

In case of a metal ($\omega_0 = 0, 4\pi f\omega_0^2 = \omega_p^2 \equiv \omega_i^2$) the power spectrum (81) depends on four parameters, the plasma frequency ω_p, the slab thickness $2a$, the electron velocity v, and the angle of incidence θ_i of the fast electron measured relative to the slab normal. In what follows the measure for the slab thickness is the dimensionless quantity $A = q_t a = a\omega_p/c$ and the electron velocity is given in units of the velocity of light, $V = v/c$. The dimensionless coupling integrals are given in units of $(e^2/\hbar c)/A$. Hence, we write

$$X_\pm(Q) = \frac{e^2}{\hbar c}\frac{1}{A} Y_\pm(Q) \tag{83}$$

and the quantities $Y_\pm(Q)$ are discussed as functions depending on A, V, θ_i.

Having discussed the reduced coupling integrals $Y_\pm(Q)$ in Sec. A, the energy-loss spectra following from them are given in Sec. B.

A. Reduced coupling integrals

The transverse-photon exchange coupling (66) and (67) of fast electrons to surface polaritons is not important at velocities usually used for electrons as an external probe for surface polaritons. Thus we give only a short account of this interaction at the end. Results in this section are given for the three electron velocities $V = 0.1$, 0.5, and 0.8, which means a kinetic energy of 2.5, 77, and 333 keV. The slab-thickness parameter is chosen to be $A = 0.5$, which means in the case of aluminium ($\hbar\omega \approx 15$ eV) a slab thickness $2a = 2Ac/\omega_p$

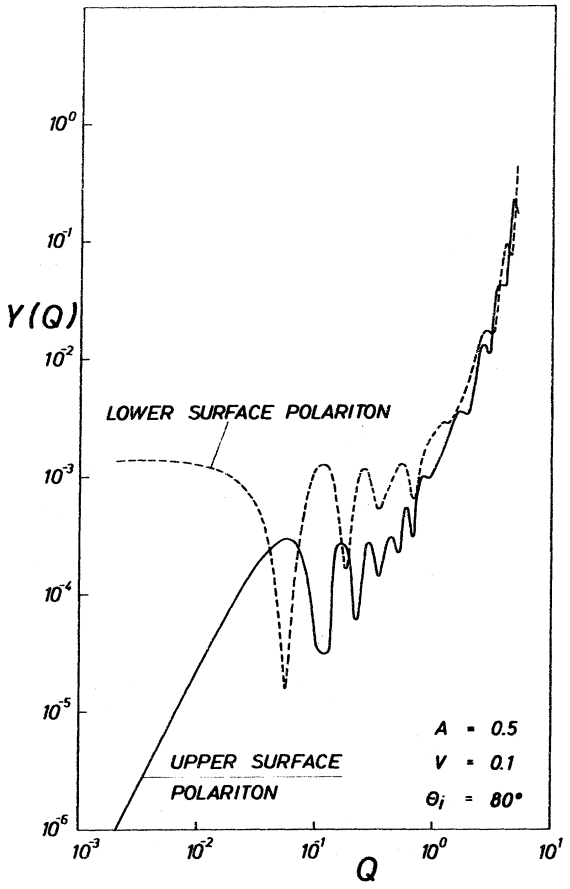

FIG. 6. The same as Fig. 5 in the case of retardation.

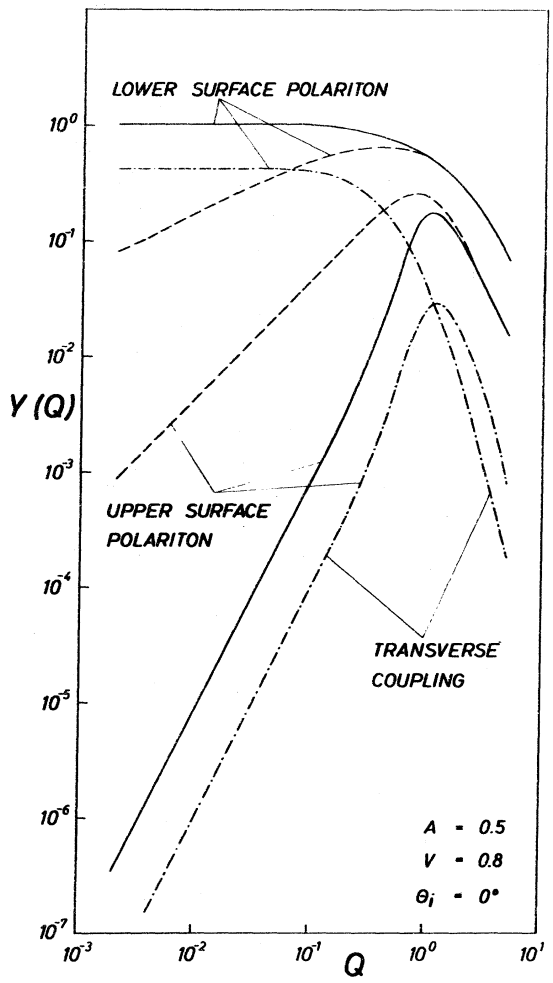

FIG. 7. Comparison of the various coupling integrals [see Eqs. (81)–(83) of text] in case of an high-energy electron. At such high energies of the incoming electron the transverse coupling defined by Eq. (66) of the text must be taken into account. The exact scattering rate contains in this case a mixed transverse-longtiudinal contribution which is not shown in the figure (for the meaning of symbols see text to Fig. 3).

≈ 133 Å. The same thickness parameters in case of heavily doped semiconductors ($\hbar\omega_p \approx 50$ meV) generate thick slabs.

Figures 3 and 4 show the coupling integrals $Y_\pm(Q)$ as defined in Eqs. (82) and (83) in the case of $V = 0.5$. The difference in retarded (continuous line) and nonretarded (broken line) scattering, respectively, is indeed quite large in the whole region $Q < 1$, $q < q_l$. The rapid change is caused by the strong difference between the retarded surface polaritons and the nonretarded surface plasmons in this region of $\vec{q}$ space.

The structures appearing at $\theta_i = 80°$ can be interpreted as "resonant" or "antiresonant" coupling of electrons to surface polaritons at a certain $\vec{q}$ vector. This behavior is caused by trigonometric functions appearing in the coupling integrals $Y_\pm(Q)$. For instance, the upper surface-polariton coupling *integrand* contains (*inter alia*) the function

$$\sin^2[(A\tan\theta_i)(Q\cos\varphi) - A/(V\cos\theta_i)\Omega_+(Q)],$$

where the azimuth φ of the $\vec{q}$ vector is measured relative to V_x with $\vec{V} = (V_x, 0, V_z)$. Depending on the parameters involved, the $\sin^2$ may or may not produce structures in the $\int_0^{2\pi} d\varphi$.

Figures 5 and 6 show the coupling integrals for $\theta_i = 80°$ in the case of $V = 0.1$. The structures compared to those in the case of $V = 0.5$ are much more pronounced. This shows clearly the sensitivity of the small-angle scattering against changes in the parameters being involved. A general feature of all these results is the strong difference in retarded and nonretarded scattering, respectively, in the case of $q < \omega_p/c$. As expected, the bigger the difference, the thicker the slab. The reason for this is quite simple. In the case of very thin slabs, the strong dispersion is mainly

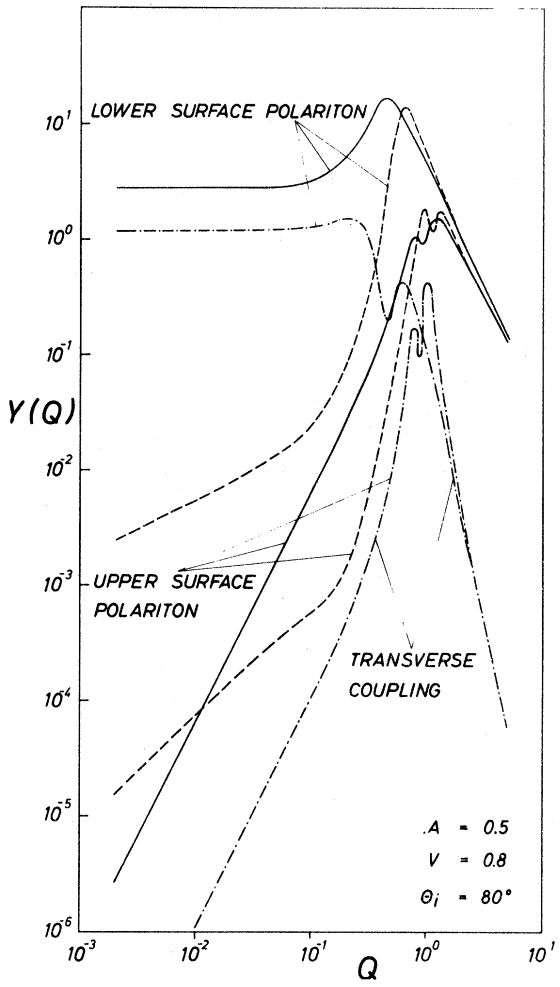

FIG. 8. The same as Fig. 7 at another θ_i. Owing to the structures at larger Q another multiple-loss spectrum is generated.

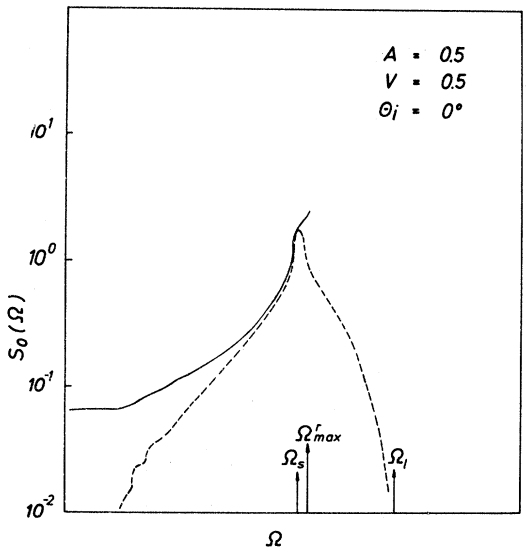

FIG. 9. Energy-loss spectrum as defined by Eq. (79) in the text. $S_0(\Omega)$ is given in units of $(2\pi\omega_p)^{-1}$, and Ω is the dimensionless frequency ω/ω_p. Continuous line: retarded spectrum; broken line: nonretarded spectrum. $\Omega_l \triangleq 1$, $\Omega_s \triangleq 1/\sqrt{2}$, and Ω^r_{max} is the reduced retarded maximum frequency of a slab with the reduced thickness $A = 0.5$. V is the velocity of the electron measured in units of c, where c is the velocity of light in vacuum. θ_i is an angle of incidence measured relative to the slab normal. The wave number q_{nd} [see Eq. (79)] beyond which the dispersion of surface excitations can be neglected is chosen to be $5\,q_l$. At this wave number the difference in the frequencies of the upper and lower surface mode is 0.5% of ω_p. Multiple scattering is unimportant and, therefore, not shown.

caused by the strong electrostatic interaction of the two surface charge densities being localized at $z = \pm a$. Switching on the interaction to photons as a competitive dispersive force is therefore only important at very small q values.

Finally, we give an example for the transverse coupling of electrons to surface polaritons. Figures 7 and 8 show results for $A = 0.5$ and $V = 0.8$. It is only at such high energies that the transverse coupling compared to the longitudinal one is of some importance and reaches the same order of magnitude. In this case, the *true* coupling of electrons to surface polaritons contains an interference or mixed term, respectively, which is not shown in the figures.

B. Retarded energy-loss spectra

In this section we discuss the multiple-loss line shape due to surface excitations on the dispersive part of surface polaritons or surface plasmons. To this end we have to calculate $S_0(\omega)$ as given by Eq. (79). The spectra are given as a function of the reduced frequency $\Omega = \omega/\omega_p$ and in units of $(2\pi\omega_p)^{-1}$.

Figure 9 shows a comparison of retarded versus nonretarded single scattering in case of $A = 0.5$, $V = 0.5$, and $\theta_i = 0°$. Multiple losses are negligibly small and not shown. The situation changes at $\theta_i = 80°$. In Figure 10 a second broad line is easily resolved. Since the multiple losses are caused by a strong coupling of high frequencies of the single-loss spectrum, *multiple scattering within the single-loss region* does not occur. For the same reason, there is a complete breakdown of the scattering rate in the region between the first and second broad line, respectively.

Another line shape is created in case of the parameters $A = 0.1$ and $V = 0.5$ (see Figs. 11 and 12). At $\theta_i = 80°$ we observe a more or less smooth connection between the first and second loss band due

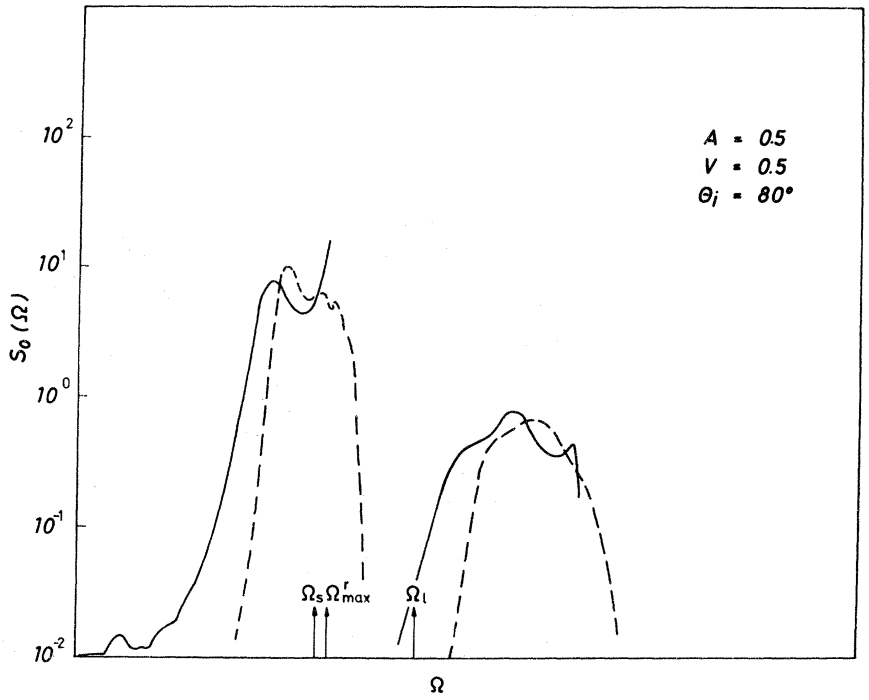

FIG. 10. The same as Fig. 9 at another θ_i. Owing to larger θ_i is a second broad band is easily resolved. It stems mainly from a dispersive double loss in the region around $Q=1$, as shown in Fig. 4.

to a combined excitation of a high-frequency surface polariton or plasmon and a low-frequency one. Because the nonretarded results are similar, they are not shown. In the case of these parameters *multiple scattering within the single-scattering region* can be observed too.

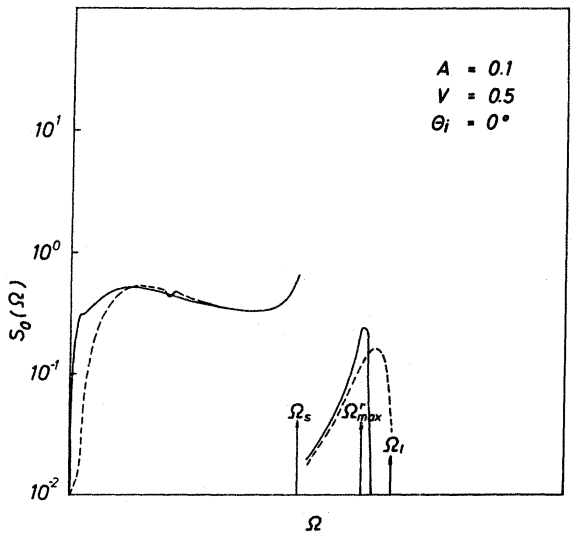

FIG. 11. Quite different dispersive single-loss spectra can be obtained as shown in this figure, compared to the spectrum shown in Fig. 9 (for the meaning of symbols see text to Fig. 9).

Finally, we give some results in case of a very thin slab, $A=0.02$, and for a relatively low kinetic energy of the electron, $V=0.02=100$ eV. Since retardation can be dropped in this case, except at very small q values, only the nonretarded results are shown. Figure 13 shows the multiple-loss spectrum at $\theta_i=67.5°$.

Comparing the scattering at small and large angles of incidence, the importance of multiple dispersive surface-loss "peaks" with increasing angle of incidence is clearly seen. A similar behavior as shown in Fig. 13 can be generated at each set of parameters. We only need to use a large angle of incidence θ_i, because this will increase the time of flight in the surface transition region of the slab.

Concerning the importance of the retarded interaction compared to the nonretarded one, the following general remarks can be made.

(1) The inelastic small-angle scattering of electrons by surface excitations can quantitatively be calculated only by taking into account the retarded nature of the modes. This is clearly demonstrated by the results shown in Figs. 3–8.

(2) The retarded coupling by "photon exchange" is unimportant at electron velocities being normally used in electron spectroscopy.

(3) Multiple scattering due to the dispersive part

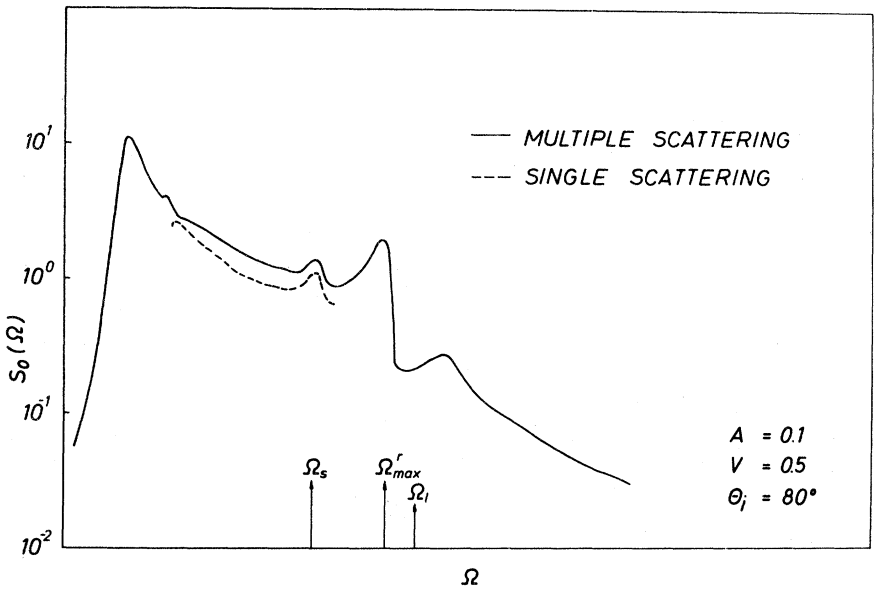

FIG. 12. Retarded multiple-loss spectrum for the parameters shown in the figure. Owing to the actual structure of the coupling integrals at small Q values multiple loss within the single-loss region is of some importance.

of the surface polariton or plasmon is an effective energy-loss channel of a fast electron, depending on the angle of incidence.

(4) Multiple scattering within the single-loss region is, in general, a small effect (see Fig. 12).

(5) The region between the different broad multiple-loss bands is sometimes smeared out (Figs. 12 and 13) and sometimes it is not (Fig. 10). It depends sensitively on the parameters A, V, and θ_i.

VI. CONCLUSION

Starting with a model Hamiltonian, the retarded coupling of electrons to the normal modes of a slab has been derived in complete analogy to the nonretarded procedure. Detailed numerical results have been given in the case of the coupling of electrons to surface polaritons in thin metal slabs. The retarded coupling is shown to be an important effect for q values being smaller than

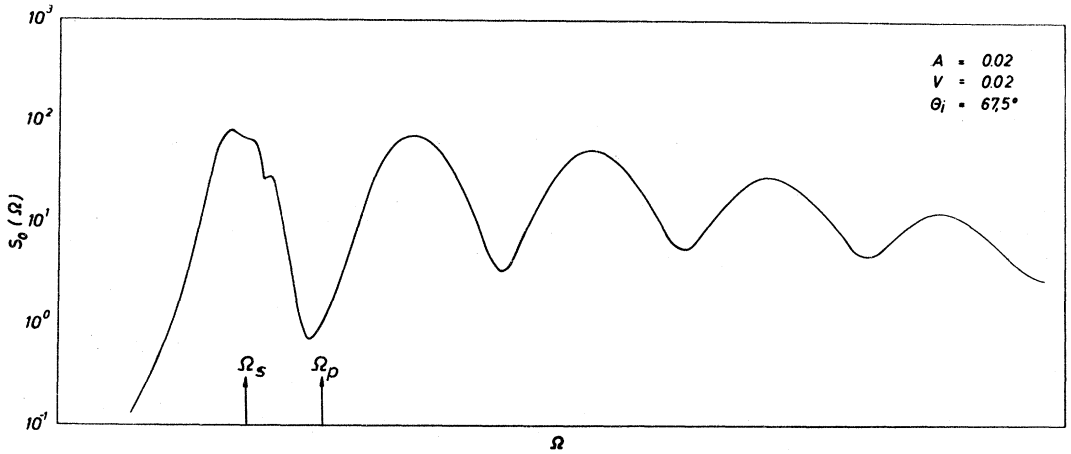

FIG. 13. Nonretarded multiple-loss spectrum for a very thin slab and a relatively-low-energy electron. Similar spectra can be generated for other parameters by a raising angle of incidence θ_i. The increasing smearing out of the region between the nth and $(n+1)$ th dispersive multiple loss is in agreement with general rules in the theory of dispersive multiple-loss line shapes.

ω_p/c.

Finally, we want to outline how to include the spatial dispersion effects. Within the phenomenological model we have to include two further terms in the Hamiltonian. Equation (1b), describing the different dispersion of transverse and longitudinal polarization waves, respectively. We derive the equations of motion and arrive at the analog of the Eqs. (8a)–(8d). These equations are then to be solved under a second boundary condition, the so-called ABC (additional boundary condition). Various ABC's can be found in the literature, especially in case of a semiconductor. Each of them produces its own surface polariton spectrum and different coupling integrals to the electron. A study following this line is underway.

ACKNOWLEDGMENT

The author is very much indebted to Professor E. Zeitler for his continuous interest and support.

[1]A. A. Lucas, E. Kartheuser, and R. G. Badro, Phys. Rev. B 2, 2488 (1970).
[2]M. Sunjić and A. A. Lucas, Phys. Rev. B 3, 719 (1971).
[3]K. L. Ngai and E. N. Economou, Phys. Rev. B 4, 2132 (1971).
[4]A. A. Lucas and M. Sunjić, Phys. Rev. Lett. 26, 229 (1971).
[5]S. Q. Wang and G. D. Mahan, Phys. Rev. B 6, 4517 (1972).
[6]P. J. Feibelman, C. B. Duke, and A. Bagchi, Phys. Rev. B 5, 2636 (1972).
[7]G. D. Mahan, in *Elementary Excitations in Solids, Molecules, and Atoms*, edited by J. T. Devreese, A. B. Kunz, and T. C. Collins (Plenum, New York, 1974), p. 93.
[8]R. Ray and G. D. Mahan, Phys. Lett. 42A, 301 (1972).
[9]M. W. Cole and M. H. Cohen, Phys. Rev. Lett. 23, 1238 (1969).
[10]J. Sak, Phys. Rev. B 6, 3981 (1972).
[11]R. M. Nieminen and C. H. Hodges, Phys. Rev. B 18, 2568 (1978).
[12]A. D'Andrea and D. Del Sole, Solid State Commun. 30, 145 (1979).
[13]W. Ekardt (unpublished).
[14]L. Schiff, *Quantum Mechanics*, 3rd ed. (McGraw-Hill, Tokyo, 1968), p. 515.
[15]R. Zeyher, C.-S. Ting, and J. Birman, Phys. Rev. B 10, 1725 (1974).
[16]S. S. Schweber, in *The Mathematics of Physics and Chemistry*, edited by H. Margenau and G. M. Murphy (Van Nostrand, New York, 1964), Vol. 2, p. 642.
[17]K. L. Kliewer and R. Fuchs, Phys. Rev. 144, 495 (1966).
[18]K. L. Kliewer and R. Fuchs, Phys. Rev. 150, 573 (1966).
[19]D. Pines, Elementary Excitations in Solids (Benjamin, New York, 1964), p. 121ff.
[20]E. N. Economou and K. L. Ngai, in *Advances in Chemical Physics* (Wiley, New York, 1974), Vol. XXVII, p. 308.